H2020-FETFLAG-2018-2021

macQsimal

Miniature Atomic vapor-Cell Quantum devices for SensIng and Metrology AppLications

Deliverable D7.1

Quantum-enhancement strategies summary

WP7 – Atomic GHz & THz sensors and vector imagers

Authors: Yongqi Shi, Philipp Treutlein (UNIBAS)

Lead participant: UNIBAS
Delivery date: 31.03.2021
Dissemination level: Public
Type: R (Document, Report)

This work has received funding from the European Union's Horizon 2020 research and innovation programme under grant agreement No. 820393.

Revision History

Author Name, Partner short name	Description	Date
Yongqi Shi (UNIBAS)	Draft 1	08.12.2020
Philipp Treutlein (UNIBAS)	Revision 1	30.12.2020
Yongqi Shi (UNIBAS)	Draft 2	28.01.2021
Philipp Treutlein (UNIBAS)	Revision 2	08.02.2021
Yongqi Shi, Philipp Treutlein (UNIBAS)	Version for Review	26.02.2021
Morgan Mitchell (ICFO)	Review comments and suggested changes	28.02.2021
Yongqi Shi, Philipp Treutlein (UNIBAS)	Final version	30.03.2021
Johannes Ripperger (accelCH)	Final formal checks and formatting	31.03.2021

Abbreviations

ARP	Adiabatic rapid passage
BAE	Back-action evasion
BEC	Bose-Einstein Condensate
CSS	Coherent spin state
EIT	Electromagnetic induced transparency
CPT	Coherent population trapping
CPW	Coplanar waveguide
MW	Microwave
PBS	Polarization beam splitter
PQS	Past quantum state
QED	Quantum Electrodynamics
QND	Quantum non-demolition
RF	Radio frequency
SERF	Spin-exchange-relaxation-free
SQL	Standard quantum limit
SSS	Spin squeezed state

Partner short names

accelCH	Accelopment Schweiz AG, CH
ICFO	Fundacio Institut de Ciencies Fotoniques, ES *(The Institute of Photonic Sciences)*
UNIBAS	Universität Basel, CH

Contents

1 OVERVIEW 6
1.1 MW sensing and detection 6
2 SUMMARY OF ATOM-BASED MW/RF DETECTION METHODS 6
2.1 Adiabatic rapid passage method 7
2.2 Rabi resonance (Atomic Candle) method 7
2.3 Rabi oscillation method 10
2.4 Parametric frequency conversion method 11
2.5 RF magnetometer 12
2.6 MW electrometry based on Rydberg atoms 13
3 SUMMARY OF QUANTUM-ENHANCED MW/RF SENSING 14
3.1 Quantum enhancement introduction 14
3.2 Scanning probe GHz magnetometer using Bose-Einstein condensates 15
3.3 MW field measurement with a mesoscopic superposition state 15
3.4 Quantum-enhanced RF magnetometers 15
3.5 Quantum enhancement on the clock transition 19
4 ROUTES TOWARDS QUANTUM-ENHANCED GHZ FIELD SENSING 20
4.1 Stroboscopic Faraday QND measurement on hyperfine transition 20
4.2 Interferometric QND measurement of hyperfine Rabi oscillations 22
5 SUMMARY 22

Executive Summary

This deliverable is a literature summary on GHz electromagnetic field sensing methods based on atomic vapor cells and potential strategies for quantum enhancement. While different GHz field sensing methods have been demonstrated using hyperfine transitions to sense the magnetic component or Rydberg transitions to sense the electric component of a GHz field, quantum enhancement has so far been demonstrated only with ultracold atoms or in the context of RF magnetometry with vapor cells. We identify QND measurements using the Faraday effect or a two-color interferometric scheme as quantum enhancement strategies that could potentially be adapted to GHz field sensing with vapor cells.

1 Overview

This deliverable is a literature summary of strategies to detect microwave (MW) magnetic fields with atomic systems (mainly atomic vapor cells) and possible strategies for quantum enhancement.

- Chapter 2 summarizes existing methods to measure the MW magnetic field via extracting the Rabi oscillation frequency of MW coupled atomic vapor.
- Chapter 3 summarizes strategies for quantum enhancement, most of which were developed in the context of radio-frequency (RF) magnetometry.
- Chapter 4 briefly points out two quantum enhancement methods that could be adapted to detect microwave magnetic fields in a single channel atomic vapor cell detector.

1.1 MW sensing and detection

Microwaves occupy a place in the electromagnetic spectrum in the frequency range between 300 MHz to 300 GHz. Microwaves are widely used in modern communication, navigation, radar, radio astronomy, industrial heating, etc. There are emerging applications of microwaves in medical imaging. Microwaves are also the basis of several emerging quantum technologies, e.g., the manipulation of ultra-cold atoms and super-conducting quantum bits.

Microwave radiation can be used to detect a target, which is usually realized by a pair of transmitting and receiving antennas, or radars. By sending a tailored MW signal and analyzing the reflected/scattered MW signal by the target, one can detect the feature/movement of the target. Sensitive detectors with small cross talk are important for this application.

A second aspect of microwave sensing is to measure the MW power at a given frequency. The key consideration in this case is the traceability of the detection method. The conventional methods include different types of calorimeters, which are usually called MW power standards.

Another type of microwave detection is to determine the frequency of an unknown microwave signal, which is usually referred to as frequency measurement or spectrum analysis.

There are mature commercial devices for detecting MW signals in different frequency ranges, which often involve some form of antenna to detect the electromagnetic field. These metallic probes can disturb the MW field to be detected. Such detectors need to be calibrated and the perturbation of the MW field by the sensor leads to systematic errors and uncertainties.

Recently, novel schemes were developed using atomic ensembles to detect and sense the MW field, which are intrinsically calibrated and some of which operate close to fundamental quantum noise limits. The rest of this deliverable mainly addresses those techniques.

2 Summary of atom-based MW/RF Detection methods

Detecting the electromagnetic field strength at MW frequencies with atoms is based on measuring the on-resonant Rabi frequency associated with the transition that the electromagnetic field drives. From the Rabi frequency, the MW field strength can be determined using well-known fundamental constants and atomic properties. There are different methods to implement this MW-driven coherent process and to measure the MW Rabi frequency.

2.1 Adiabatic rapid passage method

One of the very first ideas to use atomic systems for measuring MW field strength emerged from the need to calibrate the MW power in the early atomic frequency standards. Other than measuring the scattering parameters of a designed MW cavity, Frueholz and Camparo used adiabatic rapid passage (ARP) [1] as a coherent technique to measure the Rb atom's microwave Rabi frequency, which then directly gives the strength of the microwave field.

In a two-level atomic system, when the frequency of an electromagnetic field is swept across the resonance frequency in a speed that is "faster" than the relaxation process while "slow enough" so that the system can follow the sweep "adiabatically", there is a maximum population reversal happening which is called adiabatic rapid passage [1,2]. The maximum of the population reversal can be easily measured with a probe beam, or with the pump beam. After some theoretical calculation, Camparo [2] found that the microwave Rabi frequency (Ω_{Rabi}) is related to the microwave frequency sweep rate (β_m) that produces the maximum degree of population reversal as

$$\Omega_{\text{Rabi}}^2 \cong 1.5\beta_m.$$

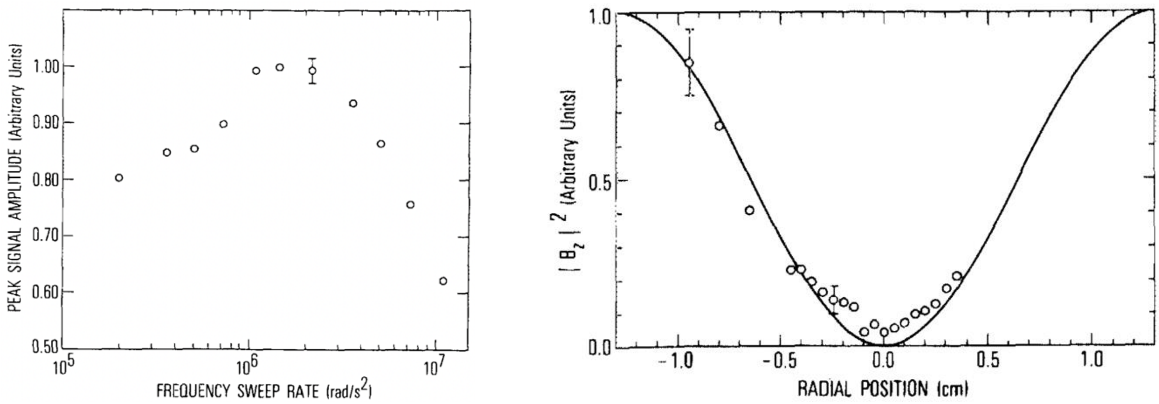

Figure 1: (left) Optical peak signal as a function of MW frequency sweep rate; (right) MW field strength distribution in radial direction. Figures adapted from [1].

The approximative description of the ARP process results in an accuracy of measuring the MW field strength of 10%-20%. As described in [1, 2], this technique allows for spatially-resolved measurements of Rabi frequencies in a MW cavity, with an accuracy limited by approximations made in modelling the ARP process.

References:

[1] Frueholz, R. P., and J. C. Camparo. "Microwave field strength measurement in a rubidium clock cavity via adiabatic rapid passage." Journal of Applied Physics 57.3 (1985): 704-708.

[2] Camparo, J. C., and R. P. Frueholz. "Parameters of adiabatic rapid passage in the 0-0 hyperfine transition of Rb 87." Physical Review A 30.2 (1984): 803.

2.2 Rabi resonance (Atomic Candle) method

Different from typical optical resonance or magnetic resonance, in which a near-resonant oscillatory field of constant amplitude, frequency and phase drives a two-level atomic system to induce Rabi oscillations, whose Rabi frequency is determined by field strength and frequency detuning, the term "Rabi resonance" refers to a dynamical enhancing resonance occurring when the coupling field is phase-modulated at half the Rabi frequency associated with the strength of the same MW field ($\omega_{pm} = \frac{1}{2}\Omega_{\text{Rabi}}$).

Rabi resonance in an atomic system was initially investigated by Cappeller and Müller [3], then was used intensively to stabilize the MW power in atomic clocks (also known as atomic candle) [4-6], to measure the absorption/refractive index [7], and to investigate the dynamical response to different phase modulation schemes, including square wave [8] and stochastic wave [9-11]).

In the last decade, exploiting its calibration-free nature, the Rabi resonance method has been utilized to realize a MW power standard [12-15], to detect the MW field inside a MW cavity [16-20], to detect the MW field from a MW horn antenna in free space [21-26], to detect a MW field with a paraffin-coated cell [27] and to perform MW magnetic field imaging [28].

The Rabi frequency is determined from the resonance in the probability to find atoms in the upper level, which depends on the phase-modulation frequency as

$$p_{\beta}^{0}(\omega_{pm}) \propto \frac{\omega_{pm}}{\sqrt{(\Omega_{Rabi}^{2} - 4\omega_{pm}^{2})^{2} + 4\gamma_{1}^{2}\omega_{pm}^{2}}}$$

This formula is derived from density matrix dynamics in the presence of the phase-modulated frequency [5]. An example of measured Rabi-resonance signals is shown in Figure 2 (from [17]).

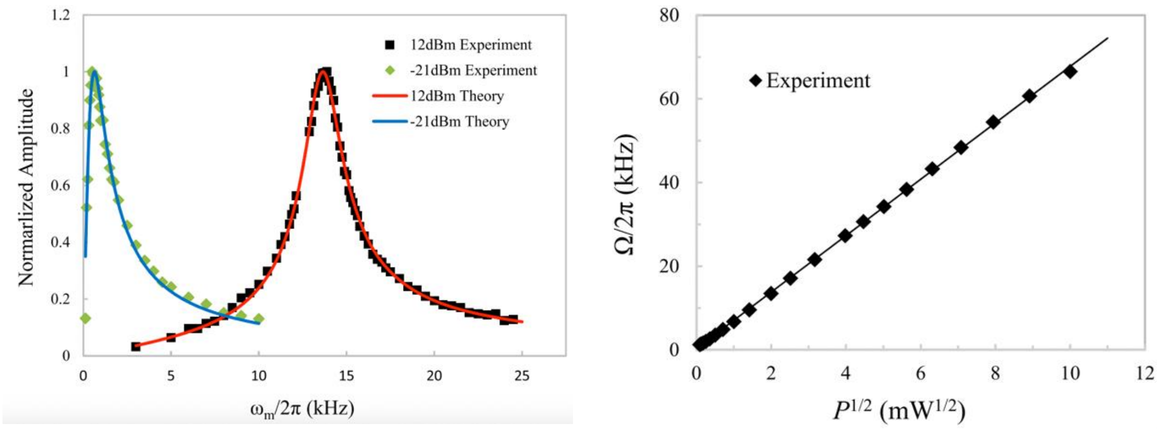

Figure 2: (Left) Optical signal measuring the upper-level population as a function of phase-modulation frequency; (Right) The extracted Rabi frequencies as a function of MW power. Figure adapted from [17].

Recently the Rabi resonance (atomic-candle) method has also been a tool to investigate the coupling between MW and cold atoms [29] and to mix the MW with the coherent population trapping (CPT) scheme [30].

References:

[3] Cappeller, U., and H. Müller. "Phasenmodulierte Anregung eines optisch gepumpten Spinsystems." AnP 497.3 (1985): 250-264.

[4] Camparo, J. C. "Atomic stabilization of electromagnetic field strength using Rabi resonances." Physical Review Letters 80.2 (1998): 222.

[5] Coffer, J. G., and J. C. Camparo. "Atomic stabilization of field intensity using Rabi resonances." Physical Review A 62.1 (2000): 013812.

[6] Coffer, J. G., et al. "Line shapes of atomic-candle-type Rabi resonances." Physical Review A 66.2 (2002): 023806.

[7] Swan-Wood, Tabitha, John G. Coffer, and James C. Camparo. "Precision measurements of absorption and refractive-index using an atomic candle." IEEE Transactions on Instrumentation and Measurement 50.5 (2001): 1229-1233.

[8] Camparo, James C., and Robert P. Frueholz. "Observation of the Rabi-resonance spectrum." Physical Review A 38.12 (1988): 6143.

[9] Frueholz, R. P., and J. C. Camparo. "Underlying simplicity of atomic population variations induced by a stochastic phase-fluctuating field." Physical Review A 54.4 (1996): 3499.

[10] Camparo, J. C., J. G. Coffer, and R. P. Frueholz. "Temporal response of an atom to a stochastic field: Resonant enhancement of population fluctuations at the Rabi frequency." Physical Review A 56.1 (1997): 1007.

[11] Camparo, J. C., J. G. Coffer, and R. P. Frueholz. "Rabi resonances induced by an off-resonant, stochastic field." Physical Review A 58.5 (1998): 3873.

[12] Kinoshita, M., K. Shimaoka, and K. Komiyama. "Rabi frequency measurement for microwave power standard using double resonance spectrum." 2008 Conference on Precision Electromagnetic Measurements Digest. IEEE, 2008.

[13] Kinoshita, Moto, Kazuhiro Shimaoka, and Koji Komiyama. "Determination of the microwave field strength using the Rabi oscillation for a new microwave power standard." IEEE Transactions on Instrumentation and Measurement 58.4 (2009): 1114-1119.

[14] Kinoshita, Moto, Kazuhiro Shimaoka, and Koji Komiyama. "Atomic microwave power standard based on the Rabi frequency." IEEE Transactions on Instrumentation and Measurement 60.7 (2010): 2696-2701.

[15] Kinoshita, Moto, Kazuhiro Shimaoka, and Yozo Shimada. "Optimization of the atomic candle signal for the precise measurement of microwave power." IEEE Transactions on Instrumentation and Measurement 62.6 (2013): 1807-1813.

[16] Sun, Fuyu, et al. "Measuring microwave cavity response using atomic Rabi resonances." Applied Physics Letters 111.5 (2017): 051103.

[17] Sun, F. Y., et al. "Rabi resonance in Cs atoms and its application to microwave magnetic field measurement." Journal of Physics Communications 2.1 (2018): 015008.

[18] Sun, Fuyu, et al. "Tunable microwave magnetic field detection based on Rabi resonance with a single cesium-rubidium hybrid vapor cell." Applied Physics Letters 113.16 (2018): 164101.

[19] Kinoshita, Moto. "Feasibility study for atomic measurement of microwave strength at arbitrary frequencies within the full X-band." 2018 Conference on Precision Electromagnetic Measurements (CPEM 2018). IEEE, 2018.

[20] Kinoshita, Moto, Yuya Tojima, and Hitoshi Iida. "Frequency extension of atomic measurement of microwave strength using Zeeman effect." IEEE Transactions on Instrumentation and Measurement 68.6 (2019): 2274-2279.

[21] Kinoshita, Moto, and Masanori Ishii. "Measurement of microwave magnetic field in free space using the Rabi frequency." 2016 Conference on Precision Electromagnetic Measurements (CPEM 2016). IEEE, 2016.

[22] Kinoshita, Moto, and Masanori Ishii. "Electromagnetic field sensor based on atomic candle." IEEE Transactions on Instrumentation and Measurement 66.6 (2017): 1592-1597.

[23] Liu, Xiaochi, et al. "Microwave magnetic field detection based on Cs vapor cell in free space." Review of Scientific Instruments 89.6 (2018): 063104.

[24] Liu, Xiaochi, et al. "Rabi resonance measurements based on CS vapor cell for microwave magnetic field detection in free space." 2018 Conference on Precision Electromagnetic Measurements (CPEM 2018). IEEE, 2018.

[25] Shi, Hao, et al. "A quantum-based microwave magnetic field sensor." Sensors 18.10 (2018): 3288.

[26] Liu, Xiaochi, et al. "Rabi Resonances in Buffer-Gas-Filled Cs-Vapor Cells for SI-Traceable Microwave Magnetic Field Detection." IEEE Transactions on Instrumentation and Measurement 69.4 (2019): 1302-1307.

[27] Ru, Ning, Xiaochi Liu, and Jifeng Qu. "Microwave magnetic field sensing based on Rabi resonance using Rb vapor cell with anti-relaxation coating." 2019 IEEE International Conference on Signal, Information and Data Processing (ICSIDP). IEEE, 2019.

[28] Liu, Xiaochi, et al. "Microwave magnetic field imaging based on Rabi resonance with an alkali-atom vapor cell." arXiv preprint arXiv:1902.06447 (2019).

[29] Tretiakov, A., and L. J. LeBlanc. "Microwave Rabi resonances beyond the small-signal regime." Physical Review A 99.4 (2019): 043402.

[30] Liu, Xiaochi, et al. "Rabi resonance in coherent population trapping: microwave mixing scheme." Optics Express 29.2 (2021): 2466-2477.

2.3 Rabi oscillation method

In a cold atom system, the absorption imaging technique and time-domain Rabi oscillation measurements on atomic hyperfine transitions were combined to demonstrate imaging of microwave magnetic field distributions near an atomic chip surface [31,32]. In a similar way, room-temperature atomic vapor cells were later used to detect [33] and image [33-36] the amplitude of a MW magnetic field. One of the prominent applications of this technique is to image the MW field distribution in a vapor cell atomic clock [37,38]. Furthermore, the MW near field distributions above coplanar-waveguide (CPW) structures have also been imaged with a tailored ultra-thin atomic vapor cell [39], with a spatial resolution of 50um*50um*140um and imaging sensitivity of $1.4\ \mu\mathrm{T}/\sqrt{\mathrm{Hz}}$. By applying a large DC magnetic field, the hyperfine transition frequency and thus the frequency range of detectable MW magnetic fields can be extended to $3\ \mathrm{GHz}{\sim}26.5\ \mathrm{GHz}$, with an accuracy of 10% [40].

The general principle of the Rabi oscillation method is to record time-domain Rabi oscillations by scanning the duration of the applied MW pulse. Once the MW frequency is calibrated to be resonant with the specific hyperfine transition (e.g., by a Ramsey measurement), the measured resonant Rabi frequency is solely dependent on the field strength of the MW polarization component driving the atomic transition and on fundamental constants. The technique can thus be used to realize an SI-traceable MW power standard, as demonstrated with a cold Cs fountain [41,42].

A typical Rabi oscillation signal measured with a miniaturized atomic vapor cell is shown below, as well as the near field distribution of a Zig-Zag CPW structure on a chip [39].

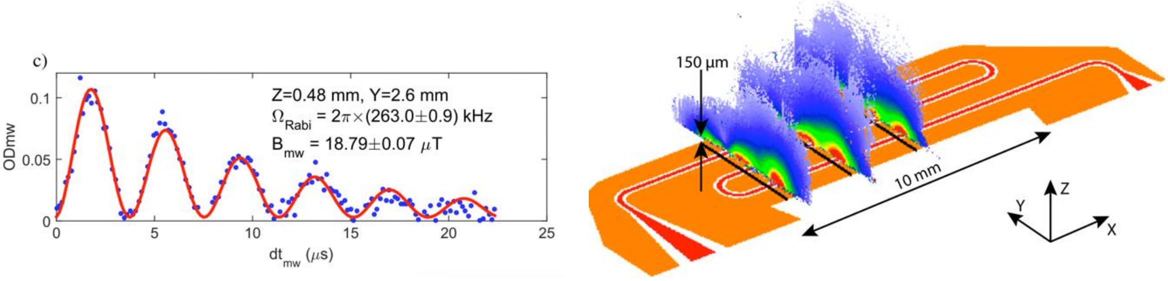

Figure 3: (Left) A typical Rabi-oscillation measurement and fitting; (Right) Measured MW near field distribution above a Zigzag CPW chip.

References:

[31] Böhi, Pascal, et al. "Imaging of microwave fields using ultracold atoms." Applied Physics Letters 97.5 (2010): 051101.

[32] Hänsch, Theodor W., et al. "Method and device for sensing microwave magnetic field polarization components." U.S. Patent No. 8,310,230. 13 Nov. 2012.

[33] Horsley, Andrew, et al. "Imaging of relaxation times and microwave field strength in a microfabricated vapor cell." Physical Review A 88.6 (2013): 063407.

[34] Böhi, Pascal, and Philipp Treutlein. "Simple microwave field imaging technique using hot atomic vapor cells." Applied Physics Letters 101.18 (2012): 181107.

[35] Böhi, Pascal, et al. "Simple microwave field imaging device." U.S. Patent No. 9,971,000. 15 May 2018.

[36] Horsley, Andrew, et al. "Spatially resolved measurement of relaxation times in a microfabricated vapor cell." 2013 Joint European Frequency and Time Forum & International Frequency Control Symposium (EFTF/IFC). IEEE, 2013.

[37] Ivanov, Anton, et al. "Experimental and numerical study of the microwave field distribution in a compact magnetron-type microwave cavity." 2014 European Frequency and Time Forum (EFTF). IEEE, 2014.

[38] Affolderbach, Christoph, et al. "Imaging the static magnetic field distribution in a vapor cell atomic clock." 2015 Joint Conference of the IEEE International Frequency Control Symposium & the European Frequency and Time Forum. IEEE, 2015.

[39] Horsley, Andrew, Guan-Xiang Du, and Philipp Treutlein. "Widefield microwave imaging in alkali vapor cells with sub-100 μm resolution." New Journal of Physics 17.11 (2015): 112002.

[40] Horsley, Andrew, and Philipp Treutlein. "Frequency-tunable microwave field detection in an atomic vapor cell." Applied Physics Letters 108.21 (2016): 211102.

[41] Crowley, Thomas P., Elizabeth A. Donley, and Thomas P. Heavner. "Quantum-based microwave power measurements: Proof-of-concept experiment." Review of Scientific Instruments 75.8 (2004): 2575-2580.

[42] Paulusse, David C., Nelson L. Rowell, and Alain Michaud. "Accuracy of an atomic microwave power standard." IEEE Transactions on Instrumentation and Measurement 54.2 (2005): 692-695.

2.4 Parametric frequency conversion method

Recently, a novel method was implemented to directly detect weak microwave signals [43] based on parametric frequency conversion [44-47]. In this method, a MW field drives the hyperfine coherence of Rb atoms at 6.8 GHz, which is converted to a polarization rotation of a probe light beam through Faraday rotation, measured by a polarimeter. Although the MW saturation limits the dynamic range of this method, it can be used to detect MW signal with a sensitivity of $1.2(1.0)$ pT/$\sqrt{\text{Hz}}$.

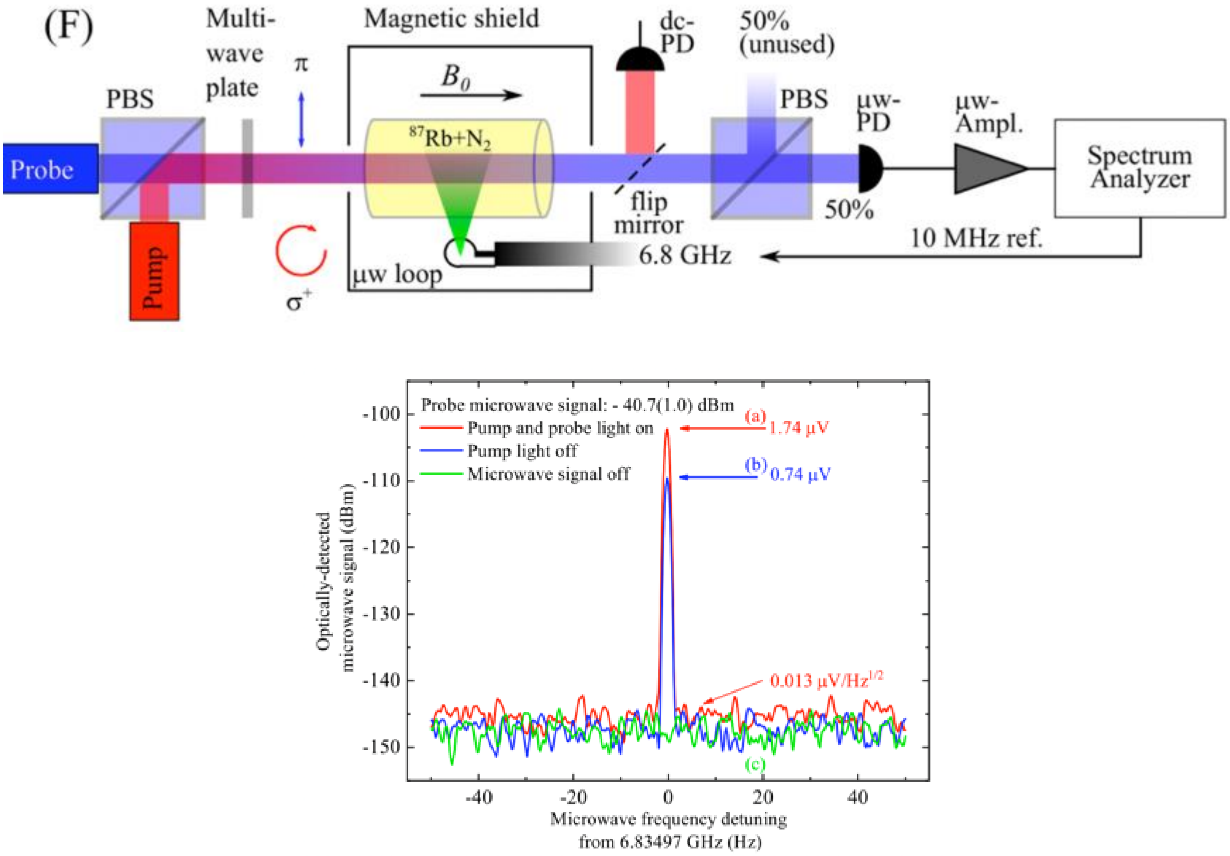

Figure 4: (Up) Setup for parametric frequency conversion method; (Down) Peak at 6.8 GHz from one arm of the PBS [43].

References:

[43] Gerginov, Vladislav, et al. "An atomic sensor for direct detection of weak microwave signals." IEEE Transactions on Microwave Theory and Techniques 67.8 (2019): 3485-3493.

[44] Firester, Arthur H., and Thomas R. Carver. "Intensity Modulation of Transmitted Light at the Ground-State Hyperfine Frequency of K 39." Physical Review 164.1 (1967): 76.

[45] Mathur, B. S., et al. "Microwave Light Modulation by an Optically Pumped Rb 87 Vapor." Physical Review Letters 21.15 (1968): 1035.

[46] Tang, H., and W. Happer. "Parametric frequency conversion of resonance radiation in optically pumped rubidium-87 vapor." Physical Review Letters 24.11 (1970): 551.

[47] Tang, H., and W. Happer. "An optically pumped parametric frequency converter." 24th Annual Symposium on Frequency Control. IEEE, 1970.

2.5 RF magnetometer

In contrast to the atom-based detection of MW fields, whose typical frequency is over 300 MHz, atom-based RF magnetometers have been developed and applied for many decades [48], operating at frequencies of typically less than 1 MHz. Generally speaking, based on the transitions between adjacent Zeeman-split magnetic sublevels at a modest static magnetic field, by measuring Faraday rotation generated by transverse components of spin polarization, the transverse RF field can be measured. With suppression of spin-exchange relaxation, the sensitivity of RF magnetometers reached $2\ \mathrm{fT}/\sqrt{\mathrm{Hz}}$ at 99 kHz [49], then $0.24\ \mathrm{fT}/\sqrt{\mathrm{Hz}}$ at 423 kHz for detecting nuclear quadrupole resonance [50]. Recently, mature RF magnetometers have been used in the application of electromagnetic induction imaging [51] and magnetic field communications and locations [52]. Techniques developed in the context of RF magnetometry, such as analysis of the spin polarization dynamics, optimization of parameters (pumping efficiency, relaxation rate, probe detuning frequency, buffer gas pressure, etc.) can be useful in developing and designing MW magnetometers based on atomic vapor cells.

References:

[48] Budker, Dmitry, and Michael Romalis. "Optical magnetometry." Nature Physics 3.4 (2007): 227-234.

[49] Savukov, Igor M., et al. "Tunable atomic magnetometer for detection of radio-frequency magnetic fields." Physical Review Letters 95.6 (2005): 063004.

[50] Lee, S-K., et al. "Subfemtotesla radio-frequency atomic magnetometer for detection of nuclear quadrupole resonance." Applied Physics Letters 89.21 (2006): 214106.

[51] Marmugi, Luca, Cameron Deans, and Ferruccio Renzoni. "Electromagnetic induction imaging with atomic magnetometers: Unlocking the low-conductivity regime." Applied Physics Letters 115.8 (2019): 083503.

[52] Gerginov, Vladislav, F. C. S. da Silva, and David Howe. "Prospects for magnetic field communications and location using quantum sensors." Review of Scientific Instruments 88.12 (2017): 125005.

2.6 MW electrometry based on Rydberg atoms

The electric field component of microwave radiation can be detected using electric dipole transitions between Rydberg states of atoms. Based on the Autler-Townes splitting of an electromagnetically-induced transparency (EIT) window in a highly excited Rydberg atom, one can detect the MW electric field amplitude. This method was initially demonstrated in a room temperature atomic vapor cell for detecting a 14 GHz electric field [52], in which the detection sensitivity is 30 μV/(cm $\sqrt{\text{Hz}}$) and the smallest detectable field is 8 μV/cm. Later, the method was used to image a 6.9 GHz MW electric field near a horn antenna as well as a CPW [53], with spatial resolution of 66 μm and electric field resolution of 50 μV/cm. With the help of homodyne readout, the sensitivity reaches 5 μV/(cm $\sqrt{\text{Hz}}$) [54] and with frequency modulation, it further improves to 3 μV/(cm $\sqrt{\text{Hz}}$) [55].

The latest remarkable result is the atomic superheterodyne receiver based on microwave-dressed Rydberg spectroscopy to detect a 6.945 GHz electric field [56], in which the electric field detection sensitivity has been improved to 55 nV/(cm $\sqrt{\text{Hz}}$).

The range of detectable frequencies has covered the millimeter range (100 GHz) [57] and by detecting strong MW electric field and continuously-tunable frequency range can be extended to ±1 GHz [58], while a large tunable range has so far not been realized.

In contrast to the Rydberg EIT-based detection technique, the optical fluorescence of Rydberg atoms induced by THz electric fields can be used to image a THz range field (0.634 THz) [58]. Using a high-speed optical camera, the speed of THz imaging has reached real-time (3 kHz) [59].

References:

[53] Sedlacek, Jonathon A., et al. "Microwave electrometry with Rydberg atoms in a vapour cell using bright atomic resonances." Nature Physics 8.11 (2012): 819-824.

[54] Fan, H. Q., et al. "Subwavelength microwave electric-field imaging using Rydberg atoms inside atomic vapor cells." Optics Letters 39.10 (2014): 3030-3033.

[55] Kumar, Santosh, et al. "Atom-based sensing of weak radio frequency electric fields using homodyne readout." Scientific Reports 7.1 (2017): 1-10.

[56] Kumar, Santosh, et al. "Rydberg-atom based radio-frequency electrometry using frequency modulation spectroscopy in room temperature vapor cells." Optics Express 25.8 (2017): 8625-8637.

[57] Jing, Mingyong, et al. "Atomic superheterodyne receiver based on microwave-dressed Rydberg spectroscopy." Nature Physics 16.9 (2020): 911-915.

[58] Gordon, Joshua A., et al. "Millimeter wave detection via Autler-Townes splitting in rubidium Rydberg atoms." Applied Physics Letters 105.2 (2014): 024104.

[59] Anderson, David A., and Georg Raithel. "Continuous-frequency measurements of high-intensity microwave electric fields with atomic vapor cells." Applied Physics Letters 111.5 (2017): 053504.

[60] Wade, Christopher G., et al. "Real-time near-field terahertz imaging with atomic optical fluorescence." Nature Photonics11.1 (2017): 40-43.

3 Summary of quantum-enhanced MW/RF sensing

This part summarizes quantum enhancement strategies for electromagnetic field sensing that were developed in the context of microwave field measurements with atomic Bose-Einstein condensates or single Rydberg atoms, or in the context of radio-frequency magnetometry with room-temperature atomic vapor cells.

3.1 Quantum enhancement introduction

Quantum noise associated with the finite number of probe particles fundamentally limits the precision and sensitivity of vapor cell electromagnetic field sensors [61-63]. On the one hand, the finite number of atoms N in the sensor gives rise to atomic projection noise $\sim 1/\sqrt{N}$, resulting in a sensitivity limit of

$$\delta B \sim \frac{\hbar}{g\mu_B}\frac{1}{\sqrt{NT\tau}}$$

for magnetic field measurements [48], often referred to as the standard quantum limit (SQL). Here, μ_B is the Bohr magneton, g is the Landé factor, T is the coherence time and τ the total integration time of the measurement. On the other hand, the finite number of photons N_{ph} in the light beam used to read out the atomic state gives rise to photon shot noise, scaling as $\sim \frac{1}{\sqrt{N_{ph}}}$. In addition, the light gives rise to measurement back-action noise $\sqrt{N_{ph}}$ perturbing the atomic state, which limits the precision at large photon numbers if the measurement is not of the quantum-non-demolition type. A number of experiments with ultracold atoms and atomic vapors have reached these noise limits and strategies to overcome them have been demonstrated [63,64]. This includes measurements with entangled probe states to reduce projection noise or shot noise, most notably spin-squeezed states of the atoms or squeezed states of light, and the implementation of quantum non-demolition measurement protocols that avoid back-action from perturbing the measurement of the quantity of interest. A variety of other quantum strategies are being explored to enhance sensitivity and precision in specific measurement tasks [63,64]. In the following, we briefly discuss result on quantum-enhanced sensing of electromagnetic fields in the MW and RF frequency range.

References:

[61] Giovannetti, Vittorio, Seth Lloyd, and Lorenzo Maccone. "Quantum-enhanced measurements: beating the standard quantum limit." Science 306.5700 (2004): 1330-1336.

[62] Giovannetti, Vittorio, Seth Lloyd, and Lorenzo Maccone. "Advances in quantum metrology." Nature Photonics 5.4 (2011): 222.

[63] Pezze, Luca, et al. "Quantum metrology with nonclassical states of atomic ensembles." Reviews of Modern Physics 90.3 (2018): 035005.

[64] Braun, Daniel, et al. "Quantum-enhanced measurements without entanglement." Reviews of Modern Physics 90.3 (2018): 035006.

3.2 Scanning probe GHz magnetometer using Bose-Einstein condensates

The first quantum-enhanced measurement of the strength of a MW field was realized with a Bose-Einstein condensate (BEC) on an atom chip [65]. A spin-squeezed state of a two-component BEC was prepared using one-axis-twisting generated by state-dependent collisions of the atoms. The spin-squeezed BEC was used to probe a 6.8 GHz magnetic field with an atom interferometric measurement scheme. By translating the position of the trapped BEC on the chip, the MW field distribution could be measured with micrometer spatial resolution. The sensitivity is $77\ \mathrm{pT}/\sqrt{\mathrm{Hz}}$ for a BEC occupying a probe volume of $20\ \mu\mathrm{m}^3$, which overcomes the standard quantum limit for the $N = 1400 \pm 40$ atoms by $4\ \mathrm{dB}$. In subsequent experiments, the performance was improved to 7 dB beyond the SQL.

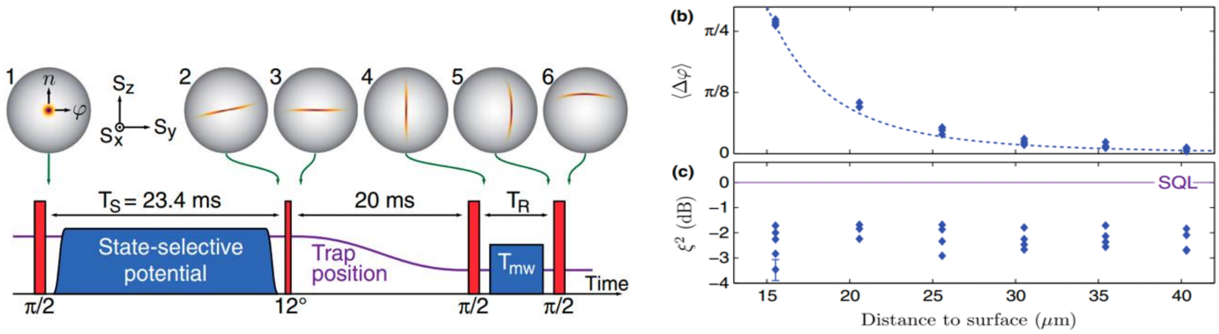

Figure 5: (Left) Experimental sequence of the MW field measurement with a spin-squeezed BEC; (Right) Phase shift due to MW field at different positions and enhancement beyond the SQL.

References:

[65] Ockeloen, Caspar F., et al. "Quantum metrology with a scanning probe atom interferometer." Physical Review Letters 111.14 (2013): 143001.

3.3 MW field measurement with a mesoscopic superposition state

In an experiment with individual Rydberg atoms strongly coupled to a superconducting microwave cavity, a mesoscopic atom-field superposition state was used for a quantum-enhanced measurement of a microwave field amplitude [66]. In this way, a microwave field at 51.5 GHz has been measured with a precision of 2.4 dB beyond the SQL.

References:

[66] Penasa, M., et al. "Measurement of a microwave field amplitude beyond the standard quantum limit." Physical Review A 94.2 (2016): 022313.

3.4 Quantum-enhanced RF magnetometers

Several schemes have been demonstrated to perform quantum enhanced measurements of radio-frequency magnetic fields. They are based on measurements of the atomic spin state with off-resonant light and involve different strategies to evade measurement back-action, to realize QND measurements and to induce measurement-based spin-squeezing.

The first scheme involves two paraffin-coated Cs vapor cells to detect an RF field at a frequency of $322\ \mathrm{kHz}$ with an amplitude of $36(3)\ \mathrm{fT}$ [67]. The atomic T_2 time is more than $30\ \mathrm{ms}$ and the total atom number is 1.5×10^{12}. By tailoring the temporal mode function of a detuned, modest power, and top-hat shape linearly-polarized probe laser pulse and performing the measurement on two oppositely spin-polarized Cs vapor cells, one can partially cancel the measurement back-action that is imposed on the collective spin by the AC stark shift from quantum noise of the probe light. The experimental sensitivity within one RF pulse is

$$\frac{B_{RF}\sqrt{\tau}}{SNR} = 0.36(4)\ \mathrm{fT}/\sqrt{\mathrm{Hz}},$$

which is just 30% above the projection-noise limited sensitivity 0.27(5) $\mathrm{fT}/\sqrt{\mathrm{Hz}}$, benefitting from the suppression of the back-action. Taking into account the full measurement cycle time, the sensitivity is

$$\frac{B_{RF}\sqrt{T}}{SNR} = 0.42(8)\ \mathrm{fT}/\sqrt{\mathrm{Hz}},$$

close to the best RF magnetometer $0.24\ \mathrm{fT}/\sqrt{\mathrm{Hz}}$ whose atom number is four-orders-of-magnitude higher [50].

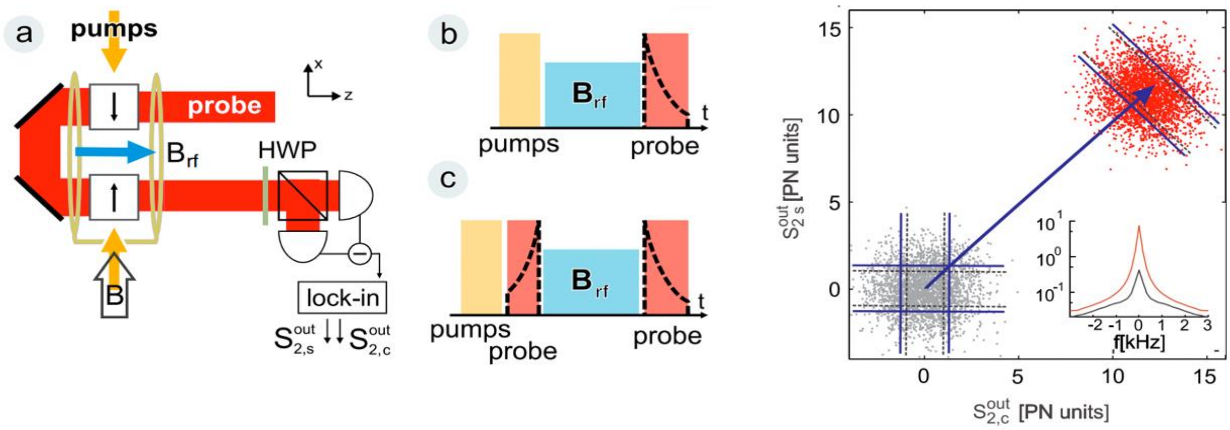

Figure 6: RF magnetometry with two oppositely polarized atomic vapor cells to suppress measurement back-action.

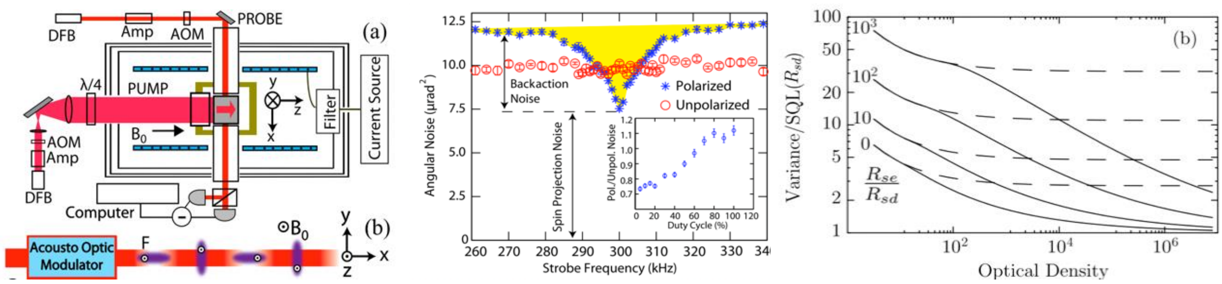

Figure 7: (Left) Schematic setup and synchronization of the measurement with the precession of the spin noise ellipse; (Middle) The evasion of back-action noise for a polarized spin system; (Right) Calculated noise levels normalized to the SQL [69].

The second scheme to evade measurement back-action is to use a stroboscopic measurement on a single cell [68-73]. By pulsing on the probe beam at twice the Larmor precession frequency, one can selectively measure only one spin component and accumulate the back-action in the orthogonal spin component, which is not measured.

By using a cell with a paraffin-coated microchannel and placing it in a cavity [70], the QND interaction rate has been massively increased and the decoherence to the environment is also mitigated. The small cross-section of the channel implies that atomic thermal motion quickly averages over the optical mode, effectively inducing a homogeneous atom-light coupling. In this case the stroboscopic measurements could reduce noise by more than $10\ \mathrm{dB}$ compared to the continuous measurement. By utilizing a two-pulse QND scheme, in which the first measurement pulse is used to squeeze the transverse spin component and the second pulse is used to read it out, a squeezing of $2.2 \pm 0.2\ \mathrm{dB}$ was observed when conditioning the second measurement on the first one. Besides, there is also a second-order tensor polarizability effect that contributes to the final squeezing performance. In this experiment [70] the RF frequency is 380 kHz and atom number is around 10^7 to 10^8.

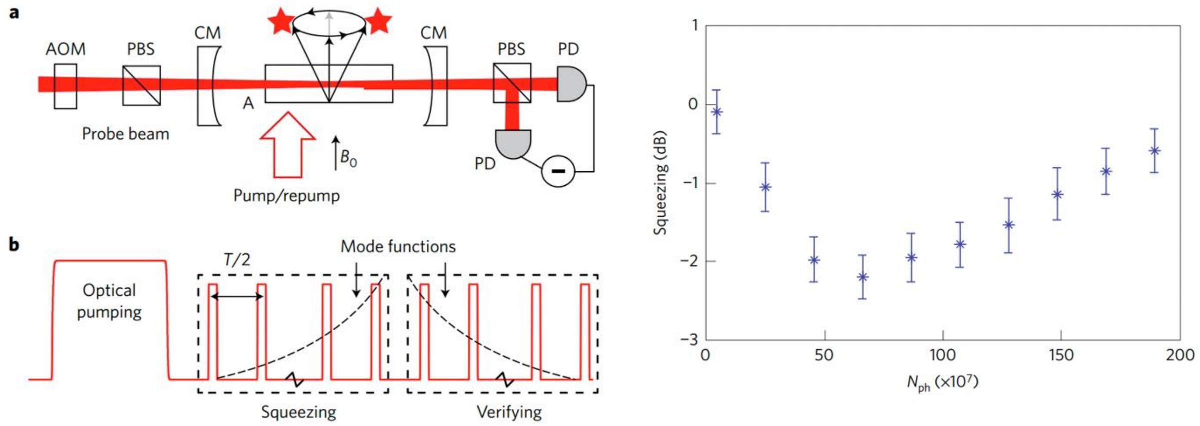

Figure 8: (Left) Cell illustration with optical cavity as well as the stroboscopic pulse sequence; (Right) Conditional squeezing in the two-pulse QND measurement scheme [70].

An interesting application of RF magnetometry is to reconstruct the waveform of an RF field. In [71] it is demonstrated that stroboscopic back-action evading measurements can be used to detect the amplitude of arbitrarily chosen components of RF waveforms in a quantum enhanced way. As an example, sinusoidal and linearly chirped waveforms were detected with a sensitivity beyond the SQL. The volume adjusted magnetic sensitivity is $\delta B\sqrt{V} \approx 3.96\ \mathrm{fT}\sqrt{\mathrm{cm}^3/\mathrm{Hz}}$, comparable with the best atomic vapor RF magnetometer. It is worth noting that this is the first work to report an improvement in RF magnetometry sensitivity by squeezing.

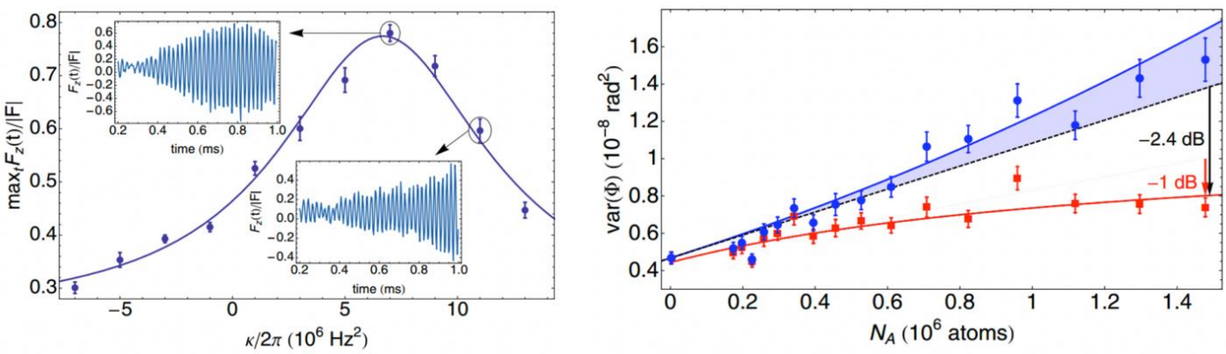

Figure 9: (Left) Response of atomic polarization to waveforms with varying frequency chirp κ; (Right) Noise scaling with atom number in comparison to the SQL [71].

Stroboscopic QND measurements can be combined with optimized data processing protocols involving both prediction and retrodiction to further decrease the noise and gain more information [72,73]. Based on the concept of the past quantum state (PQS), one such protocol uses a three-pulse scheme, in which the information gained from the middle pulse is conditioned on the first and third pulses. By using such a protocol on a paraffin-coated cell containing 1.87×10^{11} atoms for RF field sensing, a $500\ \mathrm{kHz}$ RF field was detected with a sensitivity of $32.67\ \mathrm{fT}/\sqrt{\mathrm{Hz}}$.

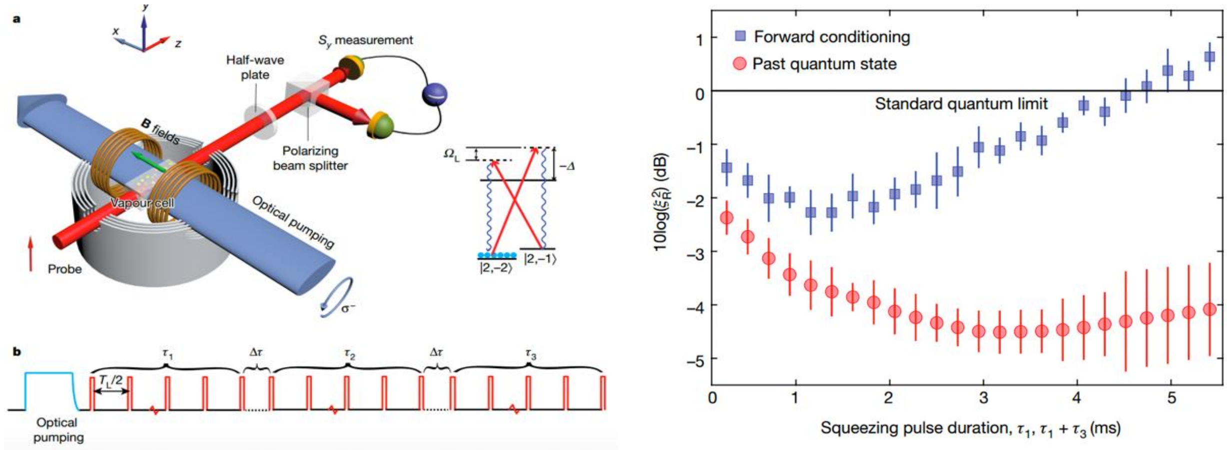

Figure 10: (Left) Experimental setup and scheme with three composite pulses; (Right) Squeezing performance comparison between two-pulse scheme (forward conditioning) and three-pulse scheme (past quantum state) [72].

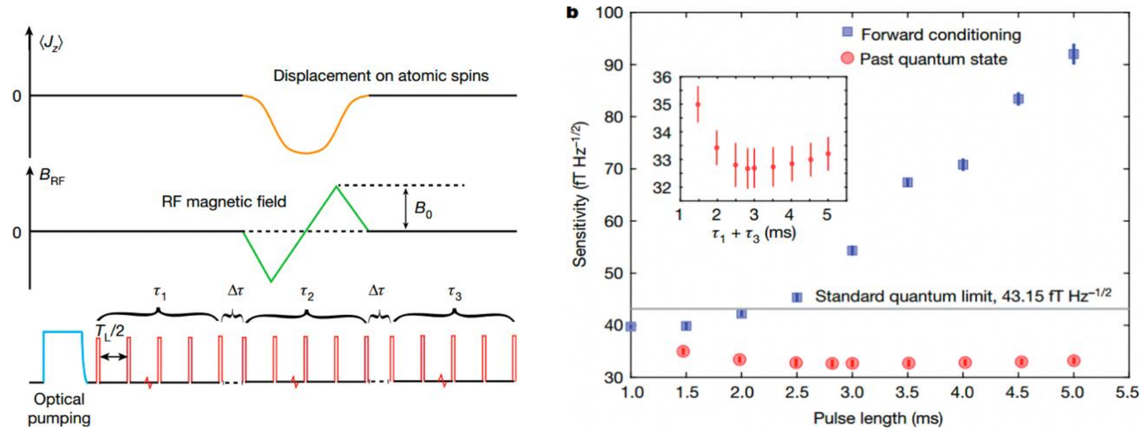

Figure 11: (Left) RF pulse shape and position; (Right) Sensitivity comparison of two-pulse scheme and three-pulse scheme with respect to SQL [72].

Another strategy to produce spin squeezing for magnetometry in atomic systems with angular momentum f > 1/2 is to exploit synthesized optical QND measurements of mixed spin alignment-orientation variables [73,74]. This technique was demonstrated to result in a 3.2 dB reduction of spin projection noise and 2.0 dB of metrologically useful squeezing in a laser-cooled atomic ensemble of atoms. Using alignment-to-orientation conversion, a magnetic field measurement was performed with a sensitivity of $105\ \mathrm{fT}/\sqrt{\mathrm{cm}^3\mathrm{Hz}}$ and a bandwidth of $200\ \mathrm{kHz}$ in a measurement volume of $3.7 \times 10^{-6}\ \mathrm{cm}^3$.

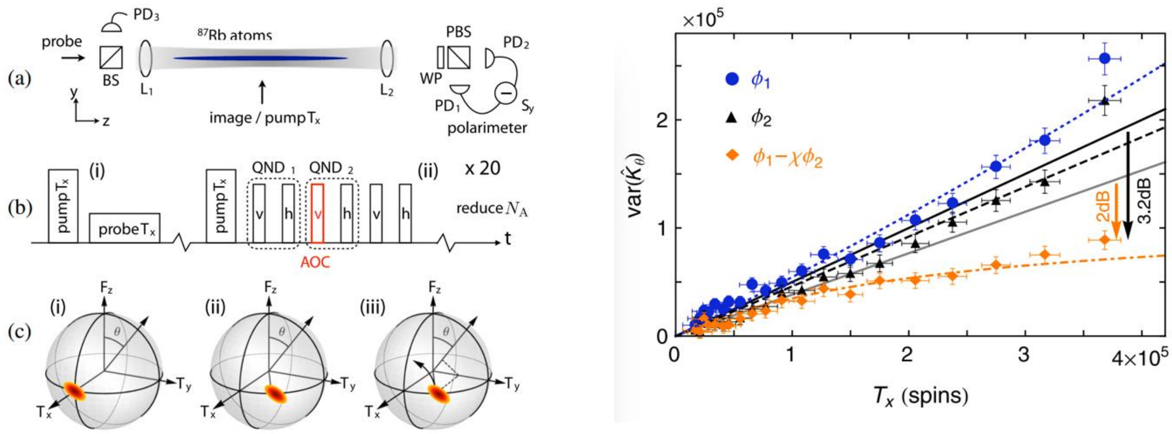

Figure 12: (Left) Setup, measurement sequences and the evolution of Tx-aligned state; (Right) Noise scaling of QND measurement for CSS and SSS [74].

References:

[67] Wasilewski, Wojciech, et al. "Quantum noise limited and entanglement-assisted magnetometry." Physical Review Letters 104.13 (2010): 133601.

[68] Shah, V., G. Vasilakis, and M. V. Romalis. “High bandwidth atomic magnetometry with continuous quantum nondemolition measurements.” Physical Review Letters 104.1 (2010): 013601.

[69] Vasilakis, G., V. Shah, and M. V. Romalis. "Stroboscopic backaction evasion in a dense alkali-metal vapor." Physical Review Letters 106.14 (2011): 143601.

[70] Vasilakis, Georgios, et al. "Generation of a squeezed state of an oscillator by stroboscopic back-action-evading measurement." Nature Physics 11.5 (2015): 389-392.

[71] Ciurana, F. Martin, et al. "Entanglement-enhanced radio-frequency field detection and waveform sensing." Physical Review Letters 119.4 (2017): 043603

[72] Bao, Han, et al. "Spin squeezing of 10^11 atoms by prediction and retrodiction measurements." Nature 581.7807 (2020): 159-163.

[73] Bao, Han, et al. "Retrodiction beyond the Heisenberg uncertainty relation." Nature Communications 11.1 (2020): 1-7.

[74] Koschorreck, M., et al. "Sub-projection-noise sensitivity in broadband atomic magnetometry." Physical Review Letters 104.9 (2010): 093602.

[75] Sewell, R. J., et al. "Magnetic sensitivity beyond the projection noise limit by spin squeezing." Physical Review Letters 109.25 (2012): 253605.

3.5 Quantum enhancement on the clock transition

QND measurements on the hyperfine clock transition of an ultracold Cs vapor in an optical dipole trap have been used for non-destructive probing of MW-driven Rabi oscillations [76], the generation of spin-squeezing [77], and the demonstration of a proof-of-principle atomic clock operating beyond the standard quantum limit [78]. In these experiments, a two-color probing scheme is used, where each of the hyperfine states is probed with a separate detuned laser beam. The atoms are placed in one arm of a Mach-Zehnder interferometer to detect the differential phase shift they induce on the two laser beams. In this way, a QND measurement of the relative population of the two clock states can be performed. Conditioned on the measurement result, a spin-squeezed state is generated and can be further manipulated with the MW field.

While these experiments used free-space laser beams for the QND measurement of the atomic state, the atom-light interaction can be enhanced using an optical cavity. In such a cavity QED system, spin-squeezing and a proof-of-principle atomic clock enhanced by spin-squeezing were reported [79], operating on the clock transition of ultracold 87Rb atoms.

References:

[76] Windpassinger, P. J., et al. "Nondestructive probing of Rabi oscillations on the cesium clock transition near the standard quantum limit." Physical Review letters 100.10 (2008): 103601.

[77] Appel, Jürgen, et al. "Mesoscopic atomic entanglement for precision measurements beyond the standard quantum limit." Proceedings of the National Academy of Sciences 106.27 (2009): 10960-10965.

[78] Louchet-Chauvet, Anne, et al. "Entanglement-assisted atomic clock beyond the projection noise limit." New Journal of Physics 12.6 (2010): 065032.

[79] Leroux, Ian D., Monika H. Schleier-Smith, and Vladan Vuletić. "Orientation-dependent entanglement lifetime in a squeezed atomic clock." Physical Review Letters 104.25 (2010): 250801.

4 Routes towards quantum-enhanced GHz field sensing

Quantum-enhanced field measurements with atomic vapor cells have so far mainly focused on measuring DC or RF magnetic fields. To perform quantum-enhanced measurements of microwave fields, it is important to identify which of the demonstrated quantum enhancement techniques summarized above could be adapted to the measurement of fields at GHz frequencies on hyperfine transitions.

4.1 Stroboscopic Faraday QND measurement on hyperfine transition

One possible approach suggesting itself is to combine Faraday rotation measurements of MW fields on atomic hyperfine transitions [43] with stroboscopic probing techniques for back-action evasion [70] in order to realize a QND measurement and create measurement-based spin-squeezing. Stroboscopic (or sinusoidally modulated) probing schemes to evade measurement back-action have by now been demonstrated with success in a number of RF magnetometry experiments, as described in section 3.4 above. While Faraday rotation at GHz frequencies on hyperfine transitions have been experimentally observed in a Rb vapor cell [43], the quantum noise limits of this technique have not yet been explored. A quantum mechanical analysis of the atom-light interaction, including effects arising from the tensor character of the atomic polarizability, will still have to be performed to analyze the feasibility of implementing such a scheme in the quantum regime. Technical challenges associated with the signal processing at GHz frequencies will also have to be addressed.

Since the maximum spin-squeezing by QND measurement is limited by the on-resonance optical depth in any single-pass geometry [80,81], we briefly estimate the on-resonance OD of the vapor cells used in different experiments on MW field detection in the classical regime [43, 34, 39] (Table 1). For comparison, we also list the corresponding experimental parameters of vapor cells used for quantum enhanced RF magnetometry [70] and measurement induced entanglement in the SERF regime [82]. We note that the quantum-enhanced RF magnetometers typically work with significantly higher OD >> 1. However, to be noted here is that the experimental conditions of the classical work in [43, 34, 39] were not optimized to obtain spin squeezing, but rather to demonstrate the principles of sensing and imaging MW magnetic fields with atomic vapor cells.

Table 1: Experimental parameters and on-resonance OD of vapor cells used for MW sensing in the classical regime and for quantum-enhanced RF magnetometry.

References	Isotope	Cell length	Buffer Gas	T	Atom density - $\mathbf{Rb^{87}}$ [1]	$\mathbf{OD_{op}^{on-res}}$
Gerginov [43]	^{87}Rb	0.38cm	N_2: 665mbar	363K	$2.44 \times 10^{12}\text{cm}^{-3}$	~1
Böhi [34]	Nat. Rb	0.3cm	Ne: 10mbar	389K	$4.22 \times 10^{12}\text{cm}^{-3}$	~18.5
Horsley [39]	Nat. Rb	0.014cm	Kr: 75mbar N_2: 25mbar	403K	$9.9 \times 10^{12}\text{cm}^{-3}$	~1.62
Vasilakis [70]	Cs	1cm	Alkene coating	300K	$1.1 \times 10^{11}\text{cm}^{-3}$	~11 ~150 (in cavity)
Kong [82]	^{87}Rb	3cm	N_2: 133mbar	463K	$3.55(6) \times 10^{14}\text{cm}^{-3}$	~5010

In order to adapt the quantum enhancement strategies based on Faraday QND measurements to the task of GHz field sensing, one can increase the on-resonance OD in a setup such as the one of [43] by increasing the cell temperature and by using a longer vapor cell, but care has to be taken to ensure that the cell is still smaller than the MW wavelength (a few cm) so that the amplitude and phase of the MW field do not differ too much across the cell. This is also one of the main technical considerations in atomic clock design for many decades. A vapor cell with a small cross section (e.g., a thin channel as in [70]) aligned parallel to the signal line of a CPW board could be used to ensure a strong and homogenous MW field in the cell. Alternatively, vapor cell atomic clock designs with a cell inside a resonator could be used [38], which are also optimized to provide a homogeneous microwave field strength across the cell.

The effective OD of the cell can be further increased with the help of an optical cavity [70,83] of moderate finesse (of order 10-20), as already demonstrated for quantum-enhanced RF magnetometers in [70]. The optimal buffer gas pressure also needs to be investigated. Overall, it seems challenging but possible to operate a setup such as the one of [43] which was used for GHz field sensing using the Faraday effect with a cell providing higher OD by a combination of longer cell length and higher cell temperature, as well as cavity enhancement of the atom-light interaction.

References.

[80] De Echaniz, S. R., et al. "Conditions for spin squeezing in a cold 87Rb ensemble." Journal of Optics B: Quantum and Semiclassical Optics 7.12 (2005): S548.

[81] Madsen, Lars Bojer, and Klaus Mølmer. "Spin squeezing and precision probing with light and samples of atoms in the Gaussian description." Physical Review A 70.5 (2004): 052324.

[82] Kong, Jia, et al. "Measurement-induced, spatially-extended entanglement in a hot, strongly-interacting atomic system." Nature communications 11.1 (2020): 1-9.

[83] Crepaz, Herbert, Li Yuan Ley, and Rainer Dumke. "Cavity enhanced atomic magnetometry." Scientific reports 5.1 (2015): 1-7.

[84] Daniel A. Steck, “Rubidium 87 D Line Data,” available online at http://steck.us/alkalidata (revision 2.2.1, 21 November 2019)

[85] Siddons, Paul, et al. "Absolute absorption on rubidium D lines: comparison between theory and experiment." Journal of Physics B: Atomic, Molecular and Optical Physics 41.15 (2008): 155004.

[1] The discrepancy in alkali vapor pressure as a function of temperature between different sources is significant (for instance, it is 25% at 300K between [84] and [85]). There are different ways to calibrate the atom numbers, e.g., using Faraday angle [70] or using the linewidth of the spin noise spectrum [82].

4.2 Interferometric QND measurement of hyperfine Rabi oscillations

Alternatively, a two-color interferometric probing scheme [76,77] could be used to detect the population difference between two sublevels belonging to the two different ground hyperfine states in order to record the Rabi oscillations driven by the MW magnetic field on the atomic hyperfine transition between them [33]. While such a measurement has been demonstrated with ultracold atoms [76,77], implementing it in a room-temperature vapor poses additional challenges. Different from the cold atom scenario, the other sublevels are also occupied to some extent and can interact with the probe light, resulting in a background and contributing noise to the signal. Good optical pumping is thus important, e.g., to one of the clock states or to an end state of the hyperfine levels. Further studies are needed to determine whether a performance comparable to the cold atom case could be achieved.

5 Summary

This deliverable summarizes GHz electromagnetic field sensing strategies based on atomic systems, mainly focusing on atomic vapor cells. Different approaches were developed using hyperfine transitions to sense the magnetic component or Rydberg transitions to sense the electric component of the MW field. Furthermore, quantum enhancement schemes are summarized, which were developed in the context of ultracold atom experiments or in the context of RF magnetometry. We point out two schemes which could be adapted for quantum-enhanced sensing of GHz magnetic fields with vapor cells.